CCS → Applied computing → Life and medical sciences → Computational biology → Biological networks

Application of Granger Causality in Decoding Covert Selective Attention with Human EEG

Weikun Niu
niuweikun518@gmail.com

Yuying Jiang
jiangyuying2017@ia.ac.cn

Yujin Zhang*
yujin.zhang@nlpr.ia.ac.cn

Xin Zhang
xzhang@nlpr.ia.ac.cn

Shan Yu*
shan.yu@nlpr.ia.ac.cn

Brainnetome Center
National Laboratory of Pattern Recognition, CAS Center for Excellence in Brain Science and Intelligence Technology, Chinese Academy of Sciences
University of Chinese Academy of Sciences
Beijing 100190, China
* Correspondence author.

ABSTRACT

Electroencephalography (EEG)-based BCIs have experienced a significant growth in recent years, especially the passive Brain Computer Interfaces (BCIs) with a wide application in the detection of cognitive and emotional states. But it is still unclear whether more subtle states, e.g., covert selective attention can be decoded with EEG signals. Here we used a behavioral paradigm to introduce the shift of selective attention between the visual and auditory domain. With EEG signals, we extracted features based on Grange Causality (GC) and successfully decoded the attentional shift through a support vector machine (SVM) based classifier. The decoding accuracy was significantly above the chance level for all 8 subjects tested. The features based on GC were further analyzed with tree-based feature importance analysis and recursive feature elimination (RFE) method to search for the optimal features for classification. Our work demonstrate that specific patterns of brain activities reflected by GC can be used to decode subtle state changes of the brain related to cross-modal selective attention, which opens new possibility of using passive BCIs in sophisticated perceptual and cognitive tasks.

Keywords

EEG; Passive BCI; Selective Attention; Granger Causality, Pattern Classification

1. INTRODUCTION

Recent years have witnessed great development in BCIs, in both fields of BCI algorithms and bio-signals acquisition technologies. One important aim of the BCIs is to utilize the brain signals of high spatial-temporal resolution in control of external devices [1]. The EEG based BCIs, by virtue of its none-invasiveness, high temporal resolution and low costs, have attracted much attention [1, 2]. The EEG based BCIs can be classified as an active or passive control modality [3-5]. In active BCIs, the user controls a device by consciously using brain signals, while in passive BCIs, the brain signals generate output without voluntary controls [4]. The passive BCIs have been applied in various fields including emotion detection and recognition of cognitive mental states such as attention and workload [6-8]. But until now, there is no evidence on the applicability of detecting the covert selective attention. The neural basis of attentional shifts between vision and audition have been studied extensively in humans with fMRI [9-11], and covert attention states such as lie detection and covert attitudes can be realized by image techniques [12]. It is still unclear whether the patterns in EEG can be recognized between audiovisual covert attention states. To answer this question will serve as an essential complement to the state of art none invasive passive BCIs. Here we designed an experimental paradigm of audiovisual covert selective attentional shift and analyzed the patterns of activities in EEG to demonstrate the applicability of passive BCI in decoding the cross-modal selective attention.

2. MATERIAL AND METHODS

2.1 Participants and Apparatus

Four males and four females aged between 21-27 (mean 25) with normal or corrected-to-normal vision and normal auditory capability participated in the experiment. All subjects provided informed written consent and were paid for their participation in the study, which was approved by the local ethics committee. EEG was recorded from a 64 electrode cap (EASYCAP), collected by Vision Recorder software (1024 Hz sampling rate), and pre-processed by BrainVision Analyzer 2.0. In addition, eye movements were recorded by ISCAN ETL-200 (240Hz sampling rate) to ensure that visual stimuli were effectively presented to the subjects. The visual stimulus was presented on a 50 cm CRT monitor (resolution 800*600, 140Hz), 60 cm away from the subject's eyes. The auditory stimuli were delivered by a headphone. Stimuli presentation was coordinated by E-Prime.

2.2 Experiment Design

The experiment of the study is a visual-auditory selective attention paradigm （Fig.1）. The subjects were presented with auditory and visual stimulus at the same time, and were instructed to respond to either one of the stimuli for each trial. The visual stimuli were 3s video clips, in which a circle with a radius of 3cm was displayed in the center of the screen. The brightness of the circle would increase, decrease or remain constant, and the subjects need to judge whether the brightness of the circle presented changed or not for visual trials. The auditory stimuli were 3s audio clips, with rising, falling, or invariant pitch. The subjects need to judge whether the pitch changed or not during auditory selective trials. The visual and auditory trails were interleaved randomly.

At first the subject should choose a difficulty level for the task. Each subject underwent three sessions of experiments, with 5-minute break in between, and each session consisted of 100 trials. In this study, we focused analysis on the time interval of 3s when subjects selectively attending the visual or auditory stimulus. We only took the correct-answered trials of each subject into analysis. The number of right answered trials of each subject (S) is as below (V: visual, A: auditory): S1 (V 120, A 139); S2 (V 145, A 113); S3 (V 115, A 125); S4 (V 102, A 133); S5 (V 112, A 132); S6 (V 142, A 113); S7 (V 123, A 124); S8 (V 110, A 105). The overall performance of all subjects were around 0.81.

2.3 Granger Causality Analysis

One electrode was used as eye movement signal, and hence this channel was excluded for the following analysis and in total we obtained the 63-channel of raw EEG data. The preprocessing steps included band pass filtering of 1-100 Hz, independent component analysis to exclude artifacts from eye movements and heart beats, and line noise removal of 50Hz, by BrainVision Analyzer 2.0 software. The data was then down sampled to 200Hz for the following Granger Causality analysis.

Two extra preprocessing steps were applied before the Granger Causality (GC) analysis. The first was to subtract the best fitting line from each time series of each channel, and the second was to remove the temporal mean of each time series to provide a zero-mean condition [13, 14]. The spectral Granger Causality was then computed by well-established method [15]. Specifically, the temporal dynamics of two time series of $X_1(t)$ and $X_2(t)$(both of length T) can be described by a bivariate autoregressive model:

$$X_1(t) = \sum_{j=1}^{p} A_{11,j} X_1(t-j) + \sum_{j=1}^{p} A_{12,j} X_2(t-j) + \xi_1(t)$$

$$X_2(t) = \sum_{j=1}^{p} A_{21,j} X_1(t-j) + \sum_{j=1}^{p} A_{22,j} X_2(t-j) + \xi_2(t)$$

where p is the maximum number of lagged observations (p<T). A contains the coefficients and ξ_1 or ξ_2 is the residuals. If the covariance of ξ_1 is reduced by the inclusion of the X_2 terms, then it is said that X_2 Granger-Causes X_1. The magnitude of the interaction can be measured by the log ratio the prediction error variances for the restricted (R) and unrestricted (U) models:

$$F_{2\to 1} = \ln \frac{\mathrm{var}(\xi_{1R(12)})}{\mathrm{var}(\xi_{1U})}$$

Since Autoregressive (AR) model might be unstable at low frequencies and near Nyquist frequency, we confined our analysis to frequencies between 5 and 50 Hz. The optimal order of AR was estimated by Akaike Information Criterion (AIC)[15, 16]. The coefficients that constituted the multi-variate AR model were then interpreted in the frequency domain [14, 17].

2.4 Coherence Analysis

For comparison, the features generated by coherence between all pairs of electrodes were tested for classification. The definition of coherence between two time series is as below [18].

$$Coh_{XY}(t,f) = \frac{< S_X(t,f) S_Y^*(t,f) >}{<| S_X(t,f)|> \bullet <| S_Y(t,f)|>}$$

where $S_X(t,f)$ and $S_Y(t,f)$ are the wavelet transforms of two zero-mean time series x(t) and y(t) respectively.

2.5 Feature Importance Analysis

Based on scikit-learn python package (https://scikit-learn.org/), the method of forest of trees module 'ExtraTreesClassifier' was used to compute the feature importance, and the optimal number of features was estimated by recursive feature elimination (RFE).

2.6 Pattern Classification

A radial basis function (RBF) based Support Vector Machine (SVM) [19] was implemented to classify the features of visual and auditory attentive trials. The classification error rate was computed by 10-fold cross validation.

3. RESULTS

We firstly searched the optimal frequency at which the auditory and the visual trials diverged maximally, and then based on each subject's optimal frequency the features were analyzed further to investigate whether there is common principles for different subjects in the audiovisual covert attention task.

3.1 The GC flow of Alpha-Beta frequency band characterizes the transition of audiovisual covert attentional state

To examine whether the audiovisual covert states can be differentiated, we firstly computed GCs across different frequencies trial by trial for each subject, and utilized GCs at a specific frequency as feature vectors for binary classification between the visual and auditory trials by a RBF-SVM (Fig. 2). We derived the distribution of classification error rate for GC features at different frequencies for each subject (Fig. 3). The SVM has the ability to classify the audio or visual trials for each subject, since the median level of the SVM's error rate is at each frequency significantly lower than the baseline level of ~0.5 (p<0.05, Wilcoxon rank sum test). This demonstrates that although the subjects were influenced by the audiovisual stimuli at the same time, there were distinct patterns revealed by GCs for the two different covert attention states. On the other hand, the optimal frequency for each subject varies from 7 to 27 Hz, which is well within the alpha-beta range. For comparison, we also used coherence between all pairs of each two electrodes as features for the same sized classifier of SVM (Fig. 4). The results of classification were considerably less accurate for each subject compared with the features used with GCs, indicating that the information flow provided by GCs is essential for characterizing the transition of covert audiovisual attention state.

3.2 The GC patterns varied substantially across each subject

In Fig.3 we showed that the classification accuracy is variable for each frequency across subjects. It remains to be answered whether the information provided by each frequency is complementary or not. To answer this question, we combined GCs from different frequencies to form new features to see if this would improve the classification performance. In Fig. 5, it is shown that the improvement resulted from the inclusion of different frequencies' GCs were very limited. Accordingly, we only took the GCs at the optimal one frequency for each subject into the following feature importance analysis.

Next, we used a tree-based method to evaluate the importance of each feature, i.e., the information flow between each of the pairs of the electrodes (Fig. 6A), and a RFE technique to search for the number of features that contributed most to the classification accuracy for each subject (Fig.6. B-I). Finally we visualized the classification hyperplane based on the optimal features to provide an intuitive picture of how the features were classified for each subject (Fig. 7). We found that the weights of the importance fluctuate considerably. The optimal features provide the highest accuracy, but the accuracy decreases with the number of features surpassing the optimal number. Additionally, the number of the optimal features varied substantially across subjects, indicating that the activity patterns across each subject varied substantially, which may be attributed to individual difference.

4. CONCLUSION

In this study, based on a novel experiment design and in-depth data analysis, we revealed that cross-modal covert attention can be decoded for each subject by EEG signals in the alpha-beta band of. By extraction GCs-based feature at the optimal frequency, we achieved the prediction accuracy far above the chance level. These results open new possibility of using passive BCIs in sophisticated perceptual and cognitive tasks. We further applied feature important analysis on these GC patterns and find substantial individual differences, suggesting the optimal classifier for decoding selective attention need to be individually customized.

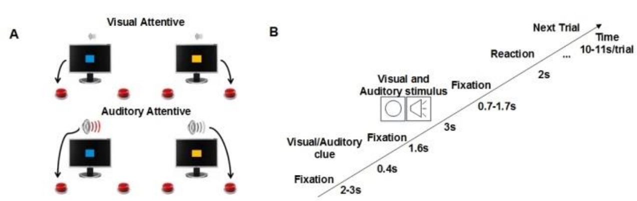

Figure 1. Illustration of the task (A) and the structure of the behavioral paradigm (B). The subject was initially presented with a clue regarding which kind of stimulus he or she should attend to for the present trial, afterwards the visual and auditory stimuli were displayed at the same time to the subject (according to the difficulty level selected for each subject). The subjects should discern whether there were any changes in the visual or the auditory stimulus by pressing the corresponding button.

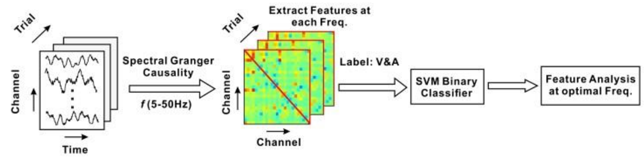

Figure 2. Data Analysis Pipeline. The data set was firstly preprocessed to zero-mean time series, and then spectral GC calculation at each frequency (between 5-50Hz, 1 Hz step) was applied and the result was the matrix with size of 63 by 63 for each trial at a specific frequency. We extracted the up-triangle part of GC matrix as the feature vector (size of 1953), and then feed to the SVM classifier for binary classification with 10-fold cross validation. The optimal frequency was observed by comparing the classification accuracy among the frequency band of 5-50 Hz, and we analyzed the feature vector at the optimal frequency for each subject.

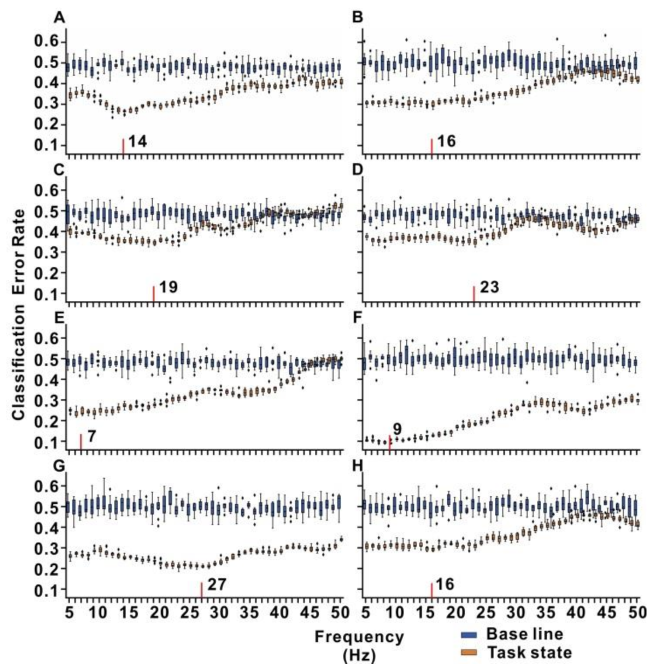

Figure 3. The pattern classification performance based on features of GC at each frequency from 5 to 50 Hz (1 Hz step). A-H, subject 1 to 8. The error rate was estimated by 10 times of 10 fold cross validation test. The red vertical bar representsthe optimal classification frequency, at which the median classification error rate is the lowest across 5-50 Hz. The blue plots, the control condition to classify trials with shuffled labels. The yellow plots, the classification of trials with original labels.

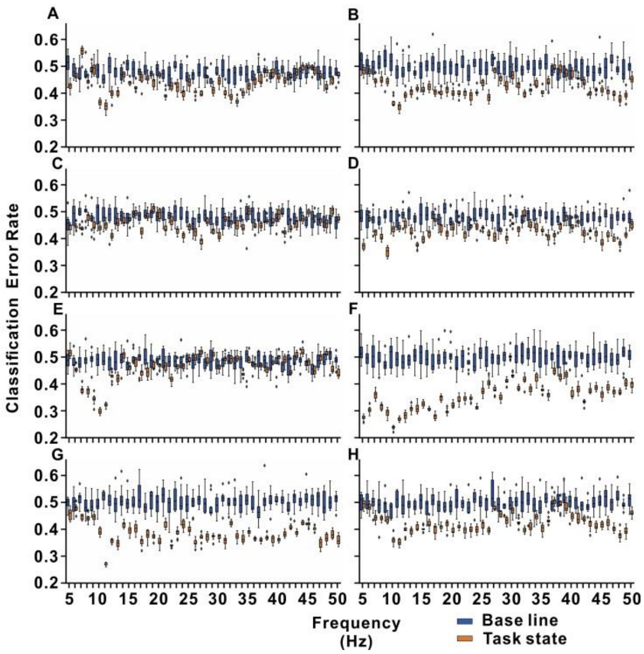

Figure 4. Classification error rate based on features of coherence between each two electrodes across 5-50Hz. A-H, subject 1-8. The error rate was calculated by 10 times of 10 fold cross validation. The blue plots, the baseline classification of trials with shuffled labels. The yellow plots, the classification of trials with original labels.

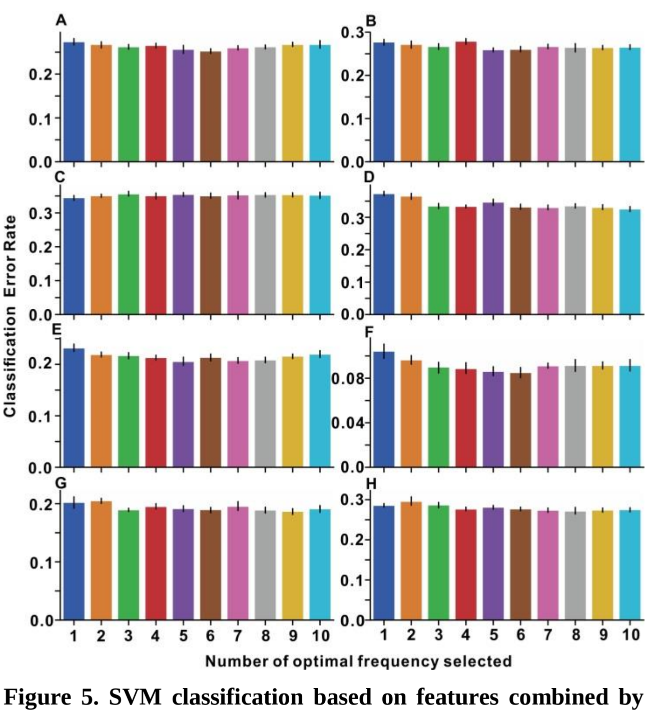

Figure 5. SVM classification based on features combined by GCs from different numbers of optimal frequencies (sorted by the classification error rate in Fig. 3). A-H, subject 1-8. The error rate was calculated by 10 times of 10 fold cross validation.

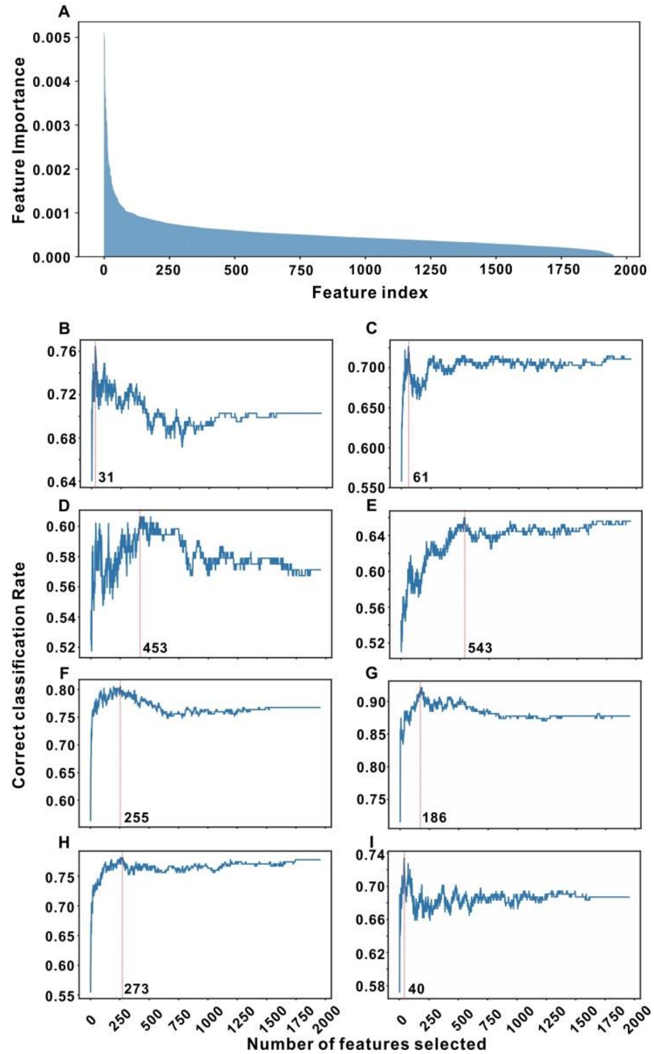

Figure 6. Feature importance and feature selection. A. Feature importance rate by tree based method for subject one at the optimal frequency of 14 Hz. Similar results were obtained for other subjects. B-I. Feature selection at the optimal frequency for subjects of 1-8. The red vertical bar represents the optimal number of features selected, which is the numbers of features associated with the best classification performance.

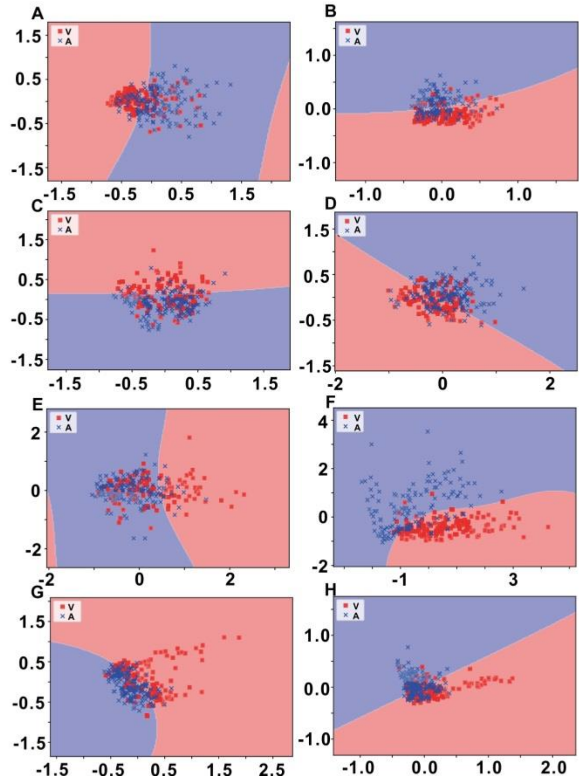

Figure 7. SVM Classification hyperplane. A-H. Subject 1-8. PCA was applied on the optimal features at the optimal frequency for each subject. In each subplot, the x axis is the first principal component, and the y axis is the second principal component. V, visual trials. A, auditory trials.

Acknowledgments: This work was supported by The National Key Research and Development Program of China (2017YFB1002502), Natural Science Foundation of China (Grant Nos. 81471368, 31571003, U1636121, and 81871398), Hundred-Talent Program of CAS (for S.Y.).

5. REFERENCES

[1] Wolpaw, J.R., et al., Brain-computer interfaces for communication and control. Clinical Neurophysiology, 2002. 113(6): p. 767-791.

[2] Abiri, R., et al., A comprehensive review of EEG-based brain-computer interface paradigms. Journal of neural engineering, 2018.

[3] Schupp, H., et al., Emotion and attention: Event-related brain potential studies. Journal of Psychophysiology, 2006. 20(2): p. 115-115.

[4] Arico, P., et al., Passive BCI beyond the lab: current trends and future directions. Physiological Measurement, 2018. 39(8): p. 19.

[5] Reichert, C., et al., A Comparative Study on the Detection of Covert Attention in Event-Related EEG and MEG Signals to Control a BCI. Frontiers in Neuroscience, 2017. 11.

[6] Blankertz, B., et al., The Berlin Brain-Computer Interface: Progress Beyond Communication and Control. Frontiers in Neuroscience, 2016. 10: p. 24.

[7] Arico, P., et al., Human Factors and Neurophysiological Metrics in Air Traffic Control: A Critical Review. IEEE reviews in biomedical engineering, 2017. 10: p. 250-263.

[8] Zander, T.O. and C. Kothe, Towards passive brain-computer interfaces: applying brain-computer interface technology to human-machine systems in general. Journal of Neural Engineering, 2011. 8(2).

[9] Shomstein, S. and S. Yantis, Control of attention shifts between vision and audition in human cortex. Journal of Neuroscience, 2004. 24(47): p. 10702-10706.

[10] Laurienti, P.J., et al., Deactivation of sensory-specific cortex by cross-modal stimuli. Journal of Cognitive Neuroscience, 2002. 14(3): p. 420-429.

[11] Sridharan, D., D.J. Levitin, and V. Menon, A critical role for the right fronto-insular cortex in switching between central-executive and default-mode networks. Proceedings of the National Academy of Sciences of the United States of America, 2008. 105(34): p. 12569-12574.

[12] Haynes, J.D. and G. Rees, Decoding mental states from brain activity in humans. Nature Reviews Neuroscience, 2006. 7(7): p. 523-534.

[13] Ding, M.Z., et al., Short-window spectral analysis of cortical event-related potentials by adaptive multivariate autoregressive modeling: data preprocessing, model validation, and variability assessment. Biological Cybernetics, 2000. 83(1): p. 35-45.

[14] Ding, M., Y. Chen, and S.L. Bressler, Granger causality: basic theory and application to neuroscience. Handbook of time series analysis: recent theoretical developments and applications, 2006: p. 437-460.

[15] Seth, A.K., A MATLAB toolbox for Granger causal connectivity analysis. Journal of Neuroscience Methods, 2010. 186(2): p. 262-273.

[16] Richter, C.G., R. Coppola, and S.L. Bressler, Top-down beta oscillatory signaling conveys behavioral context in early visual cortex. Scientific Reports, 2018. 8: p. 12.

[17] Geweke, J., MEASUREMENT OF LINEAR-DEPENDENCE AND FEEDBACK BETWEEN MULTIPLE TIME-SERIES. Journal of the American Statistical Association, 1982. 77(378): p. 304-313.

[18] Greenblatt, R.E., M.E. Pflieger, and A.E. Ossadtchi, Connectivity measures applied to human brain electrophysiological data. Journal of Neuroscience Methods, 2012. 207(1): p. 1-16.

[19] Chang, C.-C. and C.-J. Lin, LIBSVM: a library for support vector machines. ACM transactions on intelligent systems and technology (TIST), 2011. 2(3): p. 27.

Authors’ background

Your Name	Title*	Research Field	Personal website
Weikun Niu	PhD Candidate	Neuroscience, Pattern Recognition	
Yuying Jiang	Master Student	Neuroscience, Pattern Recognition	
Yujin Zhang	Associate Professor	Neuroscience, Pattern Recognition	
Xin Zhang	Associate Professor	Neuroscience, Pattern Recognition	
Shan Yu	Full Professor	Neuroscience, Pattern Recognition	http://sourcedb.ia.cas.cn/cn/iaexpert/201407/t20140717_4160162.html

***This form helps us to understand your paper better, the form itself will not be published.**

***Title can be chosen from: master student, Phd candidate, assistant professor, lecturer, senior lecturer, associate professor, full professor, research, senior research**